Author(s): Javanainen, Arto; Ferlet-Cavrois, Véronique; Bosser, Alexandre; Jaatinen, Jukka; Kettunen, Heikki; Muschitiello, Michele; Pintacuda, Francesco; Rossi, Mikko; Schwank, James R.; Shaneyfelt, Marty R.; Virtanen, Ari

Title: SEGR in SiO2-Si3N4 Stacks

Year: 2014

Version:

Please cite the original version:

Javanainen, A., Ferlet-Cavrois, V., Bosser, A., Jaatinen, J., Kettunen, H., Muschitiello, M., Pintacuda, F., Rossi, M., Schwank, J. R., Shaneyfelt, M. R., & Virtanen, A. (2014). SEGR in SiO2-Si3N4 Stacks. IEEE transactions on Nuclear Science, 61(4), 1902-1908. https://doi.org/10.1109/TNS.2014.2303493

SEGR in SiO_2–Si_3N_4 stacks

Arto Javanainen, *Member, IEEE,* Véronique Ferlet-Cavrois, *Fellow, IEEE,* Alexandre Bosser, Jukka Jaatinen, Heikki Kettunen, Michele Muschitiello, Francesco Pintacuda, Mikko Rossi, James R. Schwank, *Fellow, IEEE,* Marty R. Shaneyfelt, *Fellow, IEEE,* Ari Virtanen, *Member, IEEE*

***Abstract*—This work presents experimental Single Event Gate Rupture (SEGR) data for Metal–Insulator–Semiconductor (MIS) devices, where the gate dielectrics are made of stacked SiO_2–Si_3N_4 structures. A semi-empirical model for predicting the critical gate voltage in these structures under heavy-ion exposure is first proposed. Then interrelationship between SEGR cross-section and heavy-ion induced energy deposition probability in thin dielectric layers is discussed. Qualitative connection between the energy deposition in the dielectric and the SEGR is proposed.**

***Index Terms*—SEGR, semi-empirical, MOS, SiO_2, Si_3N_4, modeling**

I. Introduction

SINGLE Event Gate Rupture (SEGR) is a destructive event in Metal-Insulator-Semiconductor (MIS) devices induced by energetic heavy ions in biased dielectrics. Typically the phenomenon has been studied in MOSFETs with SiO_2 as the dielectric layer. Recently it has been shown that SiO_2–Si_3N_4 stack structures exhibit good resilience to Total Ionizing Dose (TID) [1]. Whereas for the SiO_2-structures a lot of research has been done concerning SEGR, the Si_3N_4-structures have remained relatively unexplored. In Ref. [2] observations on SEGR, induced by various heavy ions in SiO_2 and Si_3N_4 MIS-structures, has been reported. That study demonstrates a difference in the breakdown fields depending on the material. In Ref. [3] the dependence of SEGR on the ion energy has been studied. In that study a difference in the onset of breakdown voltages and the SEGR cross-sections has been observed in devices, irradiated with the same ion (Z_1) at the same Linear Energy Transfer (LET), but at different energy (i.e. different sides of the Bragg peak). Higher energy ions are observed to exhibit lower breakdown threshold voltage. This is called the *energy effect*.

Manuscript received September 30, 2013; revised January 28, 2014. This work has been supported by the Academy of Finland under the Finnish Centre of Excellence Programmes 2006-2011 and 2012-2017 (Project No:s 213503 and 2513553, Nuclear and Accelerator Based Physics) and European Space Agency (ESA/ESTEC Contract 18197/04/NL/CP). The portion of this work performed at Sandia National Laboratories was supported by the Defense Threat Reduction Agency under IACRO 11-4466I and the U. S. Department of Energy. Sandia National Laboratories is a multi-program laboratory managed and operated by Sandia Corporation, a wholly owned subsidiary of Lockheed Martin Corporation, for the U.S. Department of Energy's National Nuclear Security Administration under contract DE-AC04-94AL85000.

A. Javanainen, A. Bosser, J. Jaatinen, H. Kettunen, M. Rossi and A. Virtanen are with the Department of Physics, University of Jyväskylä, P.O. Box 35 (YFL), FI-40014 Jyväskylä, Finland (email: arto.javanainen@jyu.fi)

V. Ferlet-Cavrois and M. Muschitiello are with the European Space Agency, ESTEC, 2200 AG Noordwijk, The Netherlands

F. Pintacuda is with the STMicroelectronics Srl, Catania, Italy

J. R. Schwank and M. R. Shaneyfelt are with Sandia National Laboratories, Albuquerque, NM, USA

The work reported here presents experimental SEGR data for MIS-devices with SiO_2–Si_3N_4 stacks. Dielectrics with various thickness ratios have been studied. The devices have been irradiated with various heavy ions. Experimental breakdown voltages for xenon-ion-induced SEGR are shown to follow the model proposed in Ref. [4], when the intrinsic breakdown fields and the thicknesses of the corresponding dielectrics in the stack are introduced in the equations.

Possible physical mechanisms behind the SEGR are discussed in this work by comparing Geant4-simulations to experimental SEGR cross-section data. Only a qualitative picture is given here, as the exact processes in the interplay between semiconductors, metals and dielectrics, involved in the dielectric breakdown, still remains solved. Nevertheless, relative comparison of simulation results, for different structure-ion combinations, to experimental data can still give a valuable insight into what might be behind the SEGR. The qualitative model proposed here is in conjunction with the model proposed in Ref. [4]. Also similarities can be observed between simulation results presented here and the data presented in Ref. [3].

II. Experimental setup

Experiments were carried out at RADEF [5] in the University of Jyväskylä, Finland. Xenon, krypton and iron ions from the standard 9.3 MeV/u heavy-ion cocktail of RADEF were used. All the irradiations were made in vacuum. The detailed information on the ion energies and LET values in SiO_2 and Si_3N_4 are given in Table I.

There were two types of NMOS devices studied in this work, (1) capacitors and (2) powerMOS transistors. All the devices under study were manufactured by STMicroelectronics in Catania, Italy. The detailed information on the studied devices is presented in Table II. In these devices the actual gate areas, which are considered to be sensitive to SEGR, for powerMOSFETs and capacitors are $\sim$ 0.01 cm^2 and $\sim$ 0.233 mm^2, respectively. According to the manufacturer the relative uncertainty in the thicknesses of dielectric layers is $\pm 10\%$.

For obtaining the threshold voltages for SEGR, the devices voltage bias was applied on the gate while all the other connections (i.e. source and drain for MOSFETs and the bulk for capacitors) were grounded. The devices were biased in accumulation mode, i.e. transistors at negative voltages and capacitors at positive voltages. In these tests only xenon ions were used. During the irradiation the gate leakage current was monitored in order to observe the dielectric breakdown. When the leakage current reached 100 nA during ion exposure, gate

was considered broken. At any given bias the devices were exposed to ion fluences of up to $3 \cdot 10^5$ cm^{-2}, if no SEGR was observed. This fluence was considered to equal a sufficient number of ion strikes in the sensitive area in the devices (i.e. in average 3000 ions/gate for transistors and 69900 ions/gate for capacitors). If no SEGR was observed, the gate voltage was increased by one volt and device was exposed again. This was continued until SEGR occurred. The one volt increment yields an uncertainty of ± 0.5 V in the determination of the critical voltage, which was used in the error analysis. The results from this part of the experiments are presented in Section IV.

In the second part of the experiments, transistors with stacked dielectric structure of 35 nm of SiO_2 + 100 nm of Si_3N_4 (see Table II) were irradiated with Fe-, Kr- and Xe-ions. Devices were biased at their threshold voltage or above. Again, the gate current was monitored during exposure and the limit of 100 nA was used to indicate a gate rupture. The ion flux was between 5 and $5 \cdot 10^4$ ions/cm^2/s, and the total irradiation times were ranging from 5 seconds to 3 minutes. Low fluxes were used at higher voltages, in order to accurately determine the fluence where the breakdown occurs. The relative uncertainty of $\pm 10\%$ for the flux was considered, except for those low fluxes where the uncertainty derived from Poisson statistics was higher. The cumulative ion fluence for each bias condition was monitored and the beam was stopped immediately once the SEGR occurred. Thus the *fluence-to-breakdown* was obtained for each bias condition and device. One source of uncertainty in the *fluence-to-breakdown* value is due to the human reaction time from the observation of SEGR to stopping the beam. This is estimated to cause an absolute uncertainty of 2 seconds in the total irradiation time. Results from this part of the experiments are discussed in Section V.

III. Semi-empirical model

With applied bias voltage, V_{tot}, across a stacked SiO_2–Si_3N_4 MIS-structure the displacement electric field, $\vec{D}$, can be approximated with a bias dependent constant throughout the stack [12]. Hence, in each dielectric layer

$$\vec{D} = \varepsilon_0 \varepsilon_r \vec{E} = constant \propto V_{tot}, \tag{1}$$

where ε_0 is the vacuum permittivity, ε_r is the relative permittivity of the dielectric layer and $\vec{E}$ is the electric field present in the layer. Hence, it is required that $\varepsilon_r(SiO_2)\vec{E}_{SiO_2} = \varepsilon_r(Si_3N_4)\vec{E}_{Si_3N_4}$.

On the other hand the total voltage drop across the stack can be written as a sum of voltage drops across individual layers $V_{tot} = V_{SiO_2} + V_{Si_3N_4}$. Thus the electric field in each dielectric layer can be derived from the total voltage drop across the stack, by using the known thicknesses and the relative permittivities of the materials as follows

$$\begin{aligned} |\vec{E}_{SiO_2}| &\approx \frac{|V_{SiO_2}|}{t_{SiO_2}} = \frac{|V_{tot}|}{\left(t_{SiO_2} + \frac{\varepsilon_r(SiO_2)}{\varepsilon_r(Si_3N_4)} \cdot t_{Si_3N_4}\right)}, \\ |\vec{E}_{Si_3N_4}| &\approx \frac{|V_{Si_3N_4}|}{t_{Si_3N_4}} = \frac{|V_{tot}|}{\left(t_{Si_3N_4} + \frac{\varepsilon_r(Si_3N_4)}{\varepsilon_r(SiO_2)} \cdot t_{SiO_2}\right)}. \end{aligned} \tag{2}$$

Because the relative permittivities of dielectrics in MIS devices are process dependent, uncertainty of $\pm 10\%$ in these values is used for error analysis.

A model for predicting SEGR in SiO_2-based MOS-devices has been proposed in Ref. [4]. By using this model we can write the estimation for the dielectric breakdown voltage as a function of dielectric thickness, t_d, as follows

$$V_{crit}(\chi, t_{dielec}) = \frac{|\vec{E}_{int}| \cdot t_d}{1 + a \cdot (\chi)^b}, \tag{3}$$

where $a = 0.1648\ \mathrm{MeV}^{-\mathrm{b}}$ and $b = 0.25$ are the semi-empirical parameters and $|\vec{E}_{int}|$ is the intrinsic breakdown field for a given material (see values in Table I). The variable, χ (in MeV), in this model is defined as

$$\chi = LET \cdot Z_1^2 \cdot t_d \cdot \rho, \tag{4}$$

where LET is the linear energy transfer, Z_1 is the atomic number of the impinging ion and ρ is the density of the dielectric material, where the ion deposits its energy.

It is found that the critical voltage for SiO_2–Si_3N_4 stacks can be estimated from

$$V_{tot,crit} = V_{crit}(SiO_2) + V_{crit}(Si_3N_4), \tag{5}$$

where the contributions of individual dielectric layers are derived separately from Eq. (3). Thus, no other parameters are needed than those a and b in Eq. (3). The main uncertainty in the estimated critical voltage is governed by the uncertainties in the thicknesses of separate dielectric layers, which is $\pm 10\%$ for both layer materials. Thus for stacked structures the relative uncertainty for the estimated critical voltage is approximately $\pm 14\%$.

Here one should note that the relationship between individual critical voltages in Eq. (5), does not comply strictly with the requirement set by Eq. (1). Moreover, here

$$\varepsilon_r(SiO_2) \cdot \frac{V_{crit}(SiO_2)}{t_{SiO_2}} \neq \varepsilon_r(Si_3N_4) \cdot \frac{V_{crit}(Si_3N_4)}{t_{Si_3N_4}}. \tag{6}$$

This is mostly due to the fact that under intrinsic breakdown conditions the electric displacement fields, $|\vec{D}| = \varepsilon_0 \varepsilon_r |\vec{E}_{int}|$ for SiO_2 and Si_3N_4 are not equal. In the end this means that one cannot derive the total critical voltage for a stacked MIS-structure simply by estimating critical voltage for only one of the contributing layers. Both of the layers need to be considered individually. One explanation for this mismatch could be the difference in the mean energies required to generate electron-hole pairs, $\langle \epsilon_{e-h} \rangle$, in SiO_2 and Si_3N_4, which are 17 eV and 10.8 eV, respectively [7]. Hence, eventhough the LET values for heavy ions in these materials are almost the same (see Table I), the average number of ion induced electron-hole pairs per unit length, $n_{e-h} \approx \frac{LET \cdot \rho}{\langle \epsilon_{e-h} \rangle}$, is more than two times higher for Si_3N_4 than for SiO_2. Also possible differences in the electron-hole pair recombination rate in SiO_2 and Si_3N_4 can contribute the overall breakdown process of the stacked structure.

Despite of this violation of Eq. (1) in Eq. (5), the experimental data for Xe-ions, presented below, show that the model described in Eqs. (3)–(5) work with good accuracy.

IV. Experimental SEGR critical voltages

The experimental data from xenon irradiations for SEGR threshold voltages for each tested device structure are given in Table II. In this table the critical voltage, for both the experimental and the estimated, are given in absolute values, eventhough the transistors were biased at negative voltages. This is simply to illustrate the relative accuracy of the model. The table contains also the relative difference between the estimated and observed voltages. Negative percentage means that the model underestimates the breakdown threshold. The same data are presented in Fig. 1. Here in green circles the experimental breakdown voltage is divided by the total thickness of the gate stack, which represents a sort of average electric field in the dielectric layers. Additionally in this graph, the data is presented in two additional ways by plotting the estimated electric fields in the oxide and the nitride layer in the case of the breakdown as function of the thickness of the corresponding dielectric layer. The electric fields present in the separate dielectric layers are estimated by using Eg. (2). In the graph there are also the estimations for the breakdown fields in case of Xe-ions derived from Eq. (3): one for plain SiO_2 (solid blue) and another for plain Si_3N_4 (dashed red). From this graph it is obvious that in case of Xe-ions the SEGR is dominated by the nitride layer. If only the electric field in the nitride is considered the observed breakdown field is quite close to the estimated value for plain nitride layer. However, it is not possible to directly estimate the critical voltage for these structures by using solely the nitride thickness in Eq. (3). This is because there are structures with the same nitride thickness but different oxide thickness, and they exhibit different breakdown voltages. However, it was found that the observed data can be reproduced with average accuracy of $\sim$4% by using Eq. (5), where the contributions from both of the dielectric layers in the stack are taken into account. The accuracy, for all devices, is well within the uncertainty of estimated critical voltages, which is from $\pm 10\%$ to $\pm 14\%$.

The data and the estimates from Eq. (5) are presented in $t_{SiO2} - t_{Si_3N_4}$ coordinates in Fig. 2. Here the experimental

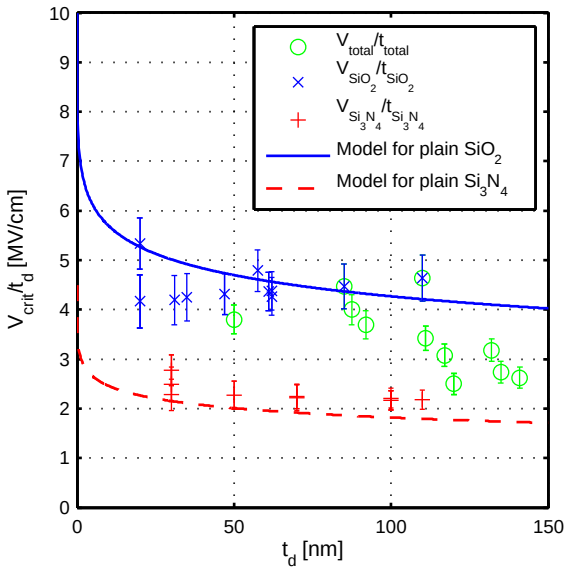

Fig. 1. The breakdown voltages across the dielectrics divided by the corresponding material thickness for Xe-ion exposure. The solid blue and dashed red lines correspond to the estimations derived from Eq. (3) for plain SiO_2 and Si_3N_4, respectively.

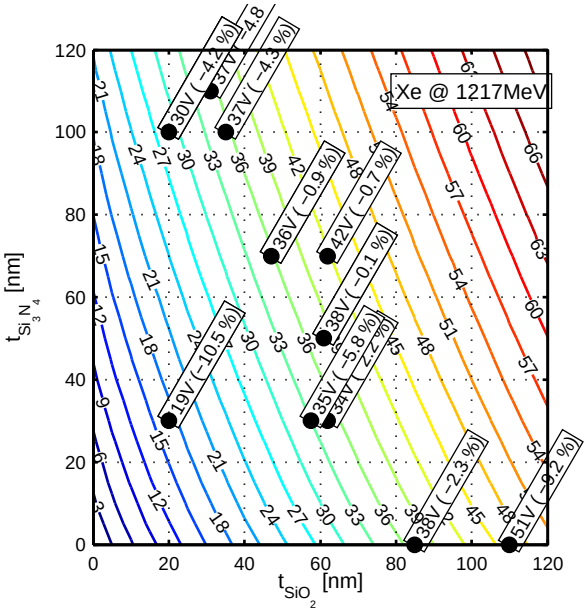

Fig. 2. 2-D contour graph of experimental (dots) and estimated (contour lines) breakdown voltages for SiO_2–Si_3N_4 stacks as a functions of material thicknesses. Abscissa and ordinate are the thicknesses for SiO_2 and Si_3N_4, respectively.

TABLE I
Material properties for SiO_2 and Si_3N_4 and the LET values, from the SRIM-code [6], in those materials for the ions considered in this work.

Material properties	**SiO_2**	**Si_3N_4**
Density, ρ [mg/cm^3]	2320	3440
Mean electron-hole generation energy [eV], (Ref. [7])	17.0	10.8
Relative permittivity, ε_r, (Ref. [8])	7.5	3.9
Intrinsic breakdown electric field, $\lvert\vec{E}_{int}\rvert$ [MV/cm]	10 (Refs. [4], [9], [10])	4.5 (Ref. [11])
LET values in MeV/(mg/cm^2), Ref. [6]	**SiO_2**	**Si_3N_4**
^{56}Fe @ 523 MeV	20.07	19.66
^{82}Kr @ 768 MeV	34.78	34.07
^{131}Xe @ 1217 MeV	65.04	63.72
^{197}Au @ 346 MeV	90.58	92.04
^{197}Au @ 2000 MeV	92.54	90.54

TABLE II

INFORMATION ON THE STRUCTURES UNDER TEST USED IN THIS WORK. ALL DEVICES ARE MANUFACTURED BY STMICROELECTRONICS, CATANIA, ITALY. ABSOLUTE VALUES FOR THE ESTIMATED AND THE OBSERVED SEGR THRESHOLD VOLTAGES FOR XENON-IRRADIATED DEVICES ARE GIVEN IN COLUMNS 6 AND 7, RESPECTIVELY. ALSO THE RELATIVE DIFFERENCE BETWEEN THE ESTIMATED AND OBSERVED VOLTAGES IS GIVEN IN THE LAST COLUMN. NEGATIVE DIFFERENCE MEANS THAT THE MODEL UNDERESTIMATES THE CRITICAL VOLTAGE.

device type	Lot	wafer	t_{SiO_2} [nm]	$t_{Si_3N_4}$ [nm]	$V_{crit,estimated}$ [V]	$V_{crit,experimental}$ [V]	difference
NMOS capacitor	3219371	15	20	100	28.7	30	-4.2 %
	3219371	20	47	70	35.7	36	-0.9 %
	3219371	25	57.5	30	33.0	35	-5.8 %
	5238004	5	110	0	46.3	51	-9.2 %
	5302642	1 and 9	61	50	38.0	38	-0.1 %
	5302642	18	31	110	35.2	37	-4.8 %
N-type powerMOSFET	3250989	5 and 10	20	30	17.0	19	-10.5 %
	3250965	3	20	100	28.7	30	-4.2 %
	3250966	2 and 12	35	100	35.4	37	-4.3 %
	3250965	17	47	70	35.7	36	-0.9 %
	3213349	8	62	30	34.8	34	2.2 %
	3250966	20	62	70	41.7	42	-0.7 %
	3213349	12	85	0	37.1	38	-2.3 %

data are presented as dots with the corresponding experimental breakdown voltage value in the box next to them. The box contains also the relative difference to the estimated value. The estimations are depicted with contours for which the estimated breakdown voltages are marked correspondingly. These results show that the model, described in Eq. (3), can be used to predict SEGR quite accurately, not only in plain SiO_2 MOS-devices, but also devices consisted of stacked SiO_2–Si_3N_4 structures. One only needs to take into account the difference in the intrinsic breakdown electric field for given dielectrics.

V. SEGR PROBABILITY

In this part the statistical aspect of the SEGR in case of different heavy ions is discussed. Fig. 3 presents the cross-section data obtained for one of the powerMOSFETs used in this work (lot: 3 250 966, wafers: 2 and 12; $t_{SiO_2} = 35$ nm and $t_{Si_3N_4} = 100$ nm). The difference in these wafers only concerns the presence (or not) of a nitride spacer. Nevertheless, they both exhibited the same breakdown threshold voltage. In this part of the tests the devices were biased above the critical voltages and the fluence-to-breakdown was recorded at several different voltages. In this part of the experiments Fe-, Kr- and Xe-ions were used (see Table I). The reciprocal of the breakdown fluence value gives the SEGR cross-section for the device at corresponding conditions (bias and radiation stress). At high voltages the SEGR cross-sections seemed to exhibit saturation at 0.01 cm^2 for Xe- and Kr-exposures, although this was not explicit. For Fe-ions the saturation was even less obvious due to low number of data points. From the information given by the manufacturer the gate area in the devices was estimated to be 0.01 cm^2, hence this value was used for saturation cross-section in the data fit, which is described later. From the graph in Fig. 3, one can see that in case of lighter ions, higher voltages are required for SEGR to occur. This is naturally expected, due to the lower LET (i.e. average energy deposition), and demonstrated e.g in Ref. [4]. The unexpected feature in the data is the slope in the transition region from the threshold to the saturation. For Xe-ions the transition is steeper than for Kr-ions. Also the data for Fe-ions seems to exhibit even more gradual transition, although there are only few data points for Fe-ions and no definite conclusion can be made.

Now we need to define the functions used in the statistical analysis of the data. The probability density function (PDF) for log-normal distribution, $f_{logn}(x)$, is defined as

$$f_{logn}(x) = \frac{1}{x \cdot \sigma_x \sqrt{2\pi}} \cdot e^{-\frac{(\ln(x)-\mu_x)^2}{2\sigma_x^2}}, \tag{7}$$

where μ_x is the mean and σ_x is the standard deviation of the natural logarithm of variable x. The actual mean for variable x in the log-normal distribution is defined as

$$\langle x \rangle = e^{\mu_x + \frac{\sigma_x^2}{2}} \tag{8}$$

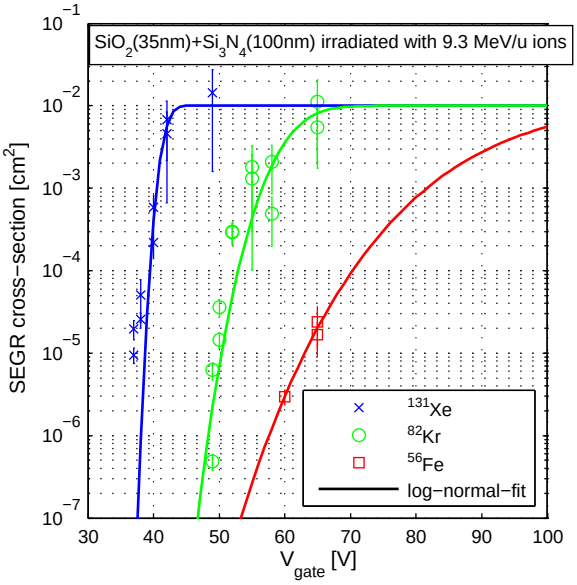

Fig. 3. SEGR cross-section data for SiO_2(35nm)-Si_3N_4(100nm) stack from Xe, Kr and Fe-irradiations as a function of gate voltage. The solid lines correspond to cumulative log-normal-fit with Eq. (10) where the distribution is scaled with $\sigma_{sat} = 10^{-2}$ cm^2. The error bars correspond to 95% confidence level.

and the statistical variance as

$$\Omega_x^2 = \left\langle (x - \langle x \rangle)^2 \right\rangle = \left(e^{\sigma_x^2} - 1 \right) e^{2\mu_x + \sigma_x^2}. \quad (9)$$

The cumulative distribution function (CDF) for log-normal distribution is defined as

$$F_{logn}(x) = \int_0^x f_{logn}(t)dt = \frac{1}{2} + \frac{1}{2} \cdot \mathrm{erf}\left(\frac{\ln(x) - \mu_x}{\sqrt{2\sigma_x^2}} \right), \quad (10)$$

where $\mathrm{erf}(x) = \frac{2}{\sqrt{\pi}} \int_0^x e^{-t^2}$ the error function. Moreover, all these can be presented by using so called complementary (or inverse) cumulative distribution function (ICDF)

$$\overline{F_{logn}(x)} = 1 - F_{logn}(x). \quad (11)$$

ICDF gives the probability that the random variable takes on a value above x.

The cross-section data in Figure 3 were fitted by using cumulative log-normal distribution, Eq. (10), and the corresponding curves from these fitting are presented also in the graph with the data. Also from the fit-curves it can be seen that more data are required for Fe-ions in order to improve the accuracy of the fit.

A. Simulations

The energy deposition in the gate dielectric layers was simulated by using Geant4-toolkit. The schematic description of the simulated geometry is presented in Fig. 4. Two types of geometries were considered, where only the sensitive layer was different. In the first case the sensitive layer was defined as 35 nm of SiO_2 + 100 nm of Si_3N_4, which corresponds to devices used for data in Fig. 3. In the other case the sensitive layer was replaced with 60 nm of SiO_2. The latter geometry corresponds to the devices used in Ref. [3], which is discussed later.

The simulation results from the first case are presented in Fig. 5. In graph (a) the simulated energy deposition spectra in stacked dielectric structure for Xe-, Kr- and Fe-ions at initial ion energy of 9.3 MeV/u are presented, and graph (b) presents the corresponding complementary cumulative probability distributions as a function of normalized energy deposition. Both graphs presents also the curve fits made by using log-normal functions, described in Eqs. (7) and (11). The parameters derived from the data fits are given in Table III.

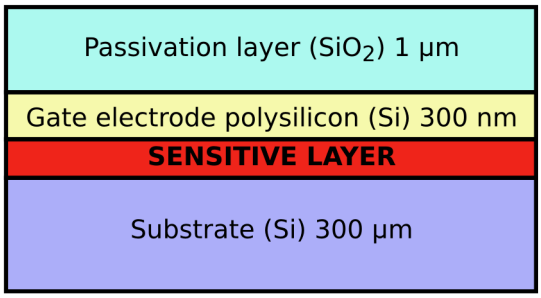

Fig. 4. The schematic cross-section of the structure used in the Geant4-simulations (not in scale). The *sensitive layer* in the simulations was either (1) 35 nm of SiO_2 + 100 nm of Si_3N_4 or (2) 60 nm of SiO_2.

For comparison, the graphs illustrate also the LET values taken from SRIM-code as well as the values for average energy deposition for each ion derived from the log-normal fit.

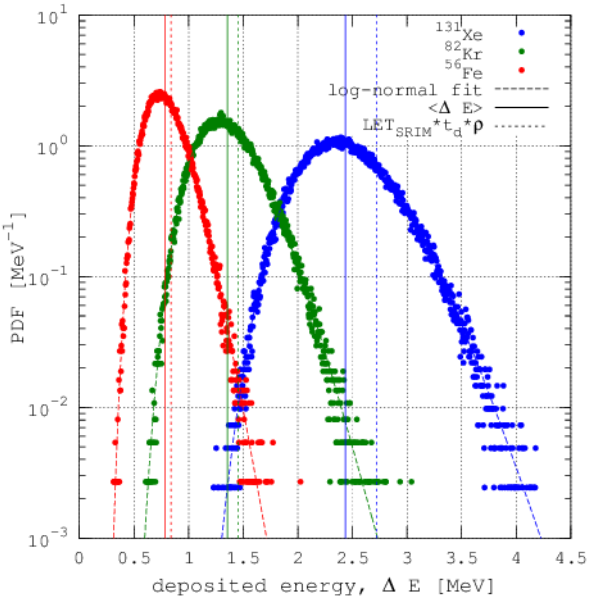

(a)

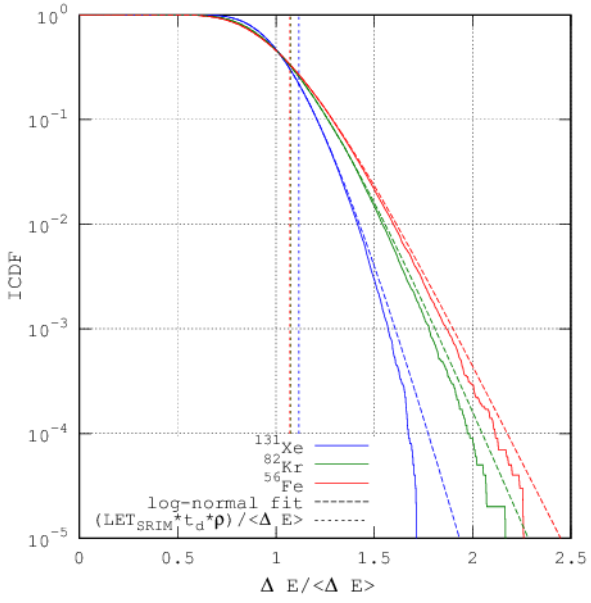

(b)

Fig. 5. Geant4-simulation results for the energy deposition in the composite SiO_2(35 nm)+Si_3N_4(100 nm) (cf. Fig. 4) sensitive layer for Xe-, Kr- and Fe-ions at initial energy of 9.3 MeV/u. Top graph presents the energy deposition spectra in solid circles with the log-normal fit in dashed line. The solid vertical lines for each ion correspond to the average energy deposition determined from the fit and the dotted vertical lines correspond to the estimated values from SRIM-code (i.e. $LET_{SiO_2} \cdot t_{SiO_2} \cdot \rho_{SiO_2} + LET_{Si_3N_4} \cdot t_{Si_3N_4} \cdot \rho_{Si_3N_4}$). In the bottom graph the same data is presented as a complementary cumulative distribution as a function of normalized energy deposition. The corresponding fitted log-normal distribution curves are also presented here with dashed lines. The dotted lines in the bottom graph represent the LET values, from SRIM-code, relative to the average Geant4-simulated energy depositions. Here the energy deposition values estimated with SRIM-code are from 7% (Fe and Kr) to 12% (Xe) higher than the values derived from Geant4 simulations.

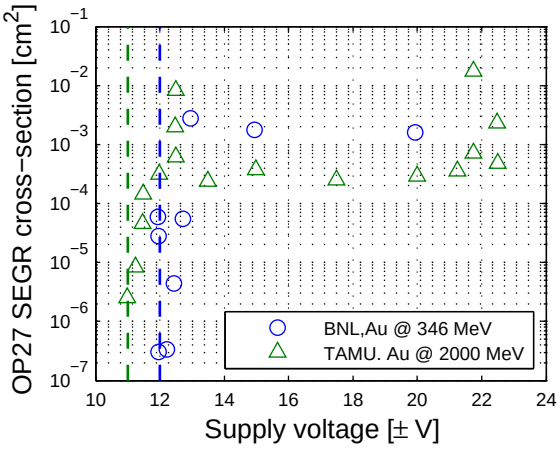

Fig. 6. SEGR cross-section data taken from Ref. [3]. The approximate SEGR threshold voltages for different Au-ion energies are marked with dashed vertical lines; right-hand line (at 11 V) for 2000 MeV and left-hand (at 12 V) for 346 MeV.

The differences in the average values for energy deposition, derived from Geant4-simulation and SRIM-code, are within 12%, for these three ions. This can be attributed mainly to the differences in the descriptions of physics in these two tools.

From the data in Fig. 5 it can be observed that the energy deposition spectra follow quite accurately the log-normal distribution. There are few aspects in these spectra which require special attention. These are the width of the distributions and the relatively high probabilities for high energy deposition events in respect to the average energy deposition. First of all there is a lot of statistical variation in the energy deposition, which would mean that the (*average*) LET values will no longer be useful when trying to describe what happens in small sensitive volumes. In addition to this, these spectra exhibit relatively high probabilities, for all three ions, for depositing more than $1.5\times$ the average energy into the sensitive layer. This is very crucial especially when considering destructive phenomena, such as SEGR.

The ICDF for the simulated data is presented as a function of normalized energy deposition, $\frac{\Delta E}{\langle \Delta E \rangle}$ in Fig. 5(b). Here $\langle \Delta E \rangle$ is the average energy deposition derived from the simulated PDF. Qualitatively, the higher energy deposition events, observed in the spectra, would require lower voltages in order to induce SEGR, which is actually what is observed in Fig. 3. This means that there could be a way to link the energy deposition to the SEGR by comparing the spectra of energy deposition in the dielectric layer of the studied MIS-device and the SEGR cross-sections. At this point this link cannot be concluded.

In order to illustrate the proposed qualitative relationship further, data from Ref. [3] are taken into a consideration. These data are presented in Fig. 6. Here the SEGR cross-sections for MOS-capacitors are plotted as a function of applied voltage across a 60 nm thick SiO_2, under exposure of Au-ions at energies of 2000 MeV and 346 MeV. At these energies, conventionally (i.e. from SRIM-code), the LET is nearly the same in SiO_2 (see Table I). Values differ only by $\sim 2\%$. Despite the seemingly similar LET values in the dielectric,

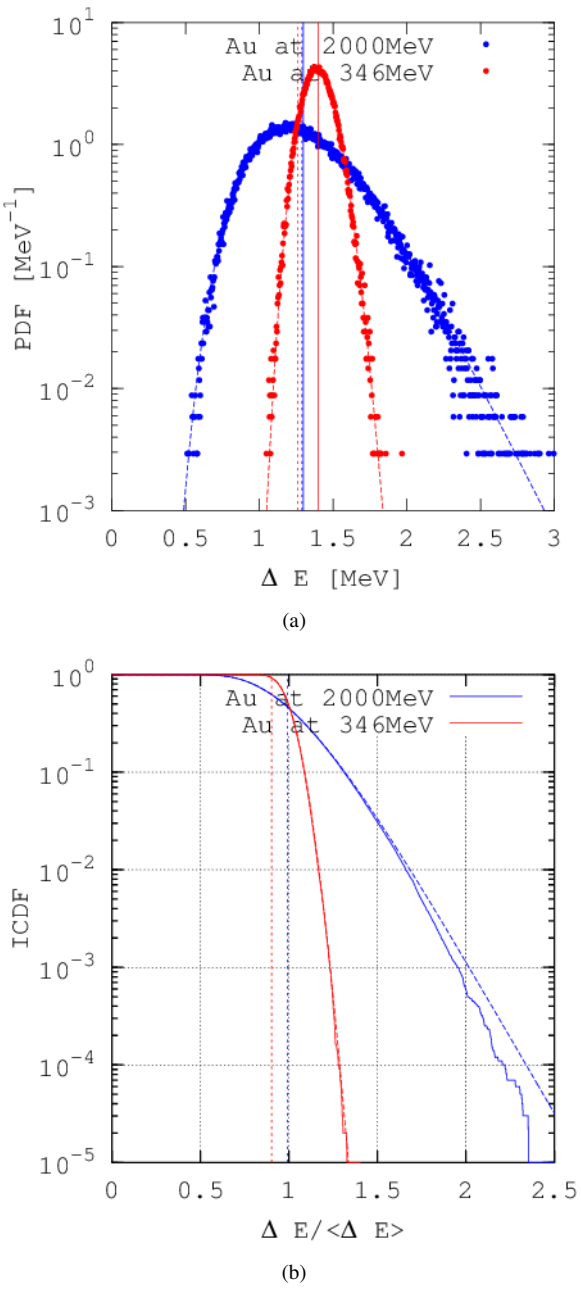

Fig. 7. Geant4-simulation results for energy deposition probability densities (top) in 60 nm thick SiO_2 for Au-ions at 2000 MeV (blue) and 346 MeV (red). The corresponding complementary cumulative distribution functions are presented in the lower graph, where the abscissa is the normalized energy deposition (cf. Fig. 5(b)).

the devices exhibit different SEGR threshold voltage as seen in Fig. 6.

Similarly to what was done above with stacked SiO_2–Si_3N_4-structure, Geant4-simulations were done in order to determine the energy deposition in this 60 nm thick SiO_2 by Au-ions at these two energies. Here, the sensitive layer in the geometry (see Fig. 4) was replaced with 60 nm thick SiO_2. Otherwise the geometry (i.e. the overlayers) was kept the same, eventhough they most likely differ from the actual devices used in Ref. [3]. Nevertheless, it can be shown that small changes in the thickness of the overlayers does not have

TABLE III
FITTING PARAMETERS FOR THE LOG-NORMAL FITTINGS PRESENTED IN FIGS. 3, 5 AND 7.

fitting parameters	SiO_2 (35 nm)+Si_3N_4(100 nm)			SiO_2 (60 nm)	
	^{56}Fe	^{82}Kr	^{131}Xe	^{197}Au @ 346 MeV	^{197}Au @ 2000 MeV
$\mu_{V_{gate}}$	4.585	4.118	3.733	–	–
$\sigma_{V_{gate}}$	0.143	0.064	0.025	–	–
$\langle V_{gate} \rangle\,[V]$	99.06	61.54	41.83	–	–
$\Omega_{V_{gate}}[V]$	14.24	3.96	1.067	–	–
$\Omega_{V_{gate}} / \langle V_{gate} \rangle\,[\%]$	14	6.4	2.5	–	–
$\mu_{\Delta E}$	-0.266	0.284	0.878	0.3328	0.234
$\sigma_{\Delta E}$	0.215	0.198	0.157	0.0685	0.236
$\langle \Delta E \rangle\,[MeV]$	0.784	1.355	2.436	1.398	1.298
$\Omega_{\Delta E}[MeV]$	0.171	0.271	0.386	0.096	0.311
$\Omega_{\Delta E} / \langle \Delta E \rangle\,[\%]$	22	20	16	7	24

major impact on the shape of the energy deposition [4].

For these two ion energies the Geant4-simulations, indeed, exhibit very different energy deposition spectra. The simulation results for 60 nm-thick SiO_2 are presented in Fig. 7. Here both (a) the PDF as a function of energy deposition, as well as (b) the ICDF as a function of normalized energy deposition are given similarly to Fig. 5. Fig. 7 also presents the curves from the log-normal fitting for ion energies. The fitting parameters are tabulated in Table III. Similarly to what was observed from Fig. 5, also here the averages for energy deposition from the Geant4-simulations and SRIM-code differ by a maximum of 10%. This can be considered as a good agreement taking into account the overall uncertainties in the dielectric thicknesses in real target structures.

The distinctive feature in the spectra here is that, for Au-ions at 2000 MeV the spectrum extends to higher energy deposition values, which would, in practice, mean lower SEGR threshold voltage, just like it is observed in Fig. 6. By looking at the energy deposition spectra and the SEGR data here, one can see the similarities to what was discussed above, in case of the stacked SiO_2–Si_3N_4 structure.

In order to verify the proposed interrelationship between SEGR and the energy deposition, more experimental SEGR cross-section data would be needed and they should be carefully compared with similar simulations presented here, and/or theoretical considerations including energy loss straggling.

VI. CONCLUSIONS

This work shows that the model, proposed in Ref. [4], for predicting critical voltage for SEGR works also well for MIS devices with SiO_2–Si_3N_4 stacked structures. This supports the hypotheses that the statistical variation in the heavy-ion energy deposition (i.e. the *straggling*) plays a role in the observed SEGR. Indeed more qualitative evidence is presented in this paper by showing similarities in the energy deposition spectra in thin dielectrics, simulated with Geant4, and experimental SEGR cross-section data. However, at this point the exact physical mechanisms underlying the SEGR remain still unsolved. Nevertheless, these findings give a direction where the future research of SEGR should be aimed at in order to explain the phenomenom better.

REFERENCES

[1] G. Bo, L. Gang, W. Li-Xin, H. Zheng-Sheng, S. Li-Mei, Z. Yan-Fei, T. Rui, and W. Hai-Zhou, "Radiation damage effects on power VDMOS devices with composite SiO_2-Si_3N_4 films," *Chin. Phys. B*, vol. 22, no. 3, p. 36103, 2013.

[2] T. F. Wrobel, "On heavy-ion induced hard-errors in dielectric structures," *IEEE Trans. Nucl. Sci*, vol. 34, no. 6, pp. 1262 –1268, dec. 1987.

[3] G. K. Lum, N. Boruta, J. M. Baker, L. Robinette, M. R. Shaneyfelt, J. R. Schwank, P. E. Dodd, and J. A. Felix, "New experimental findings for single-event gate rupture in MOS capacitors and linear devices," *IEEE Trans. Nucl. Sci*, vol. 51, no. 6, pp. 3263–3269, 2004.

[4] A. Javanainen, V. Ferlet-Cavrois, J. Jaatinen, H. Kettunen, M. Muschitiello, F. Pintacuda, M. Rossi, J. R. Schwank, M. R. Shaneyfelt, and A. Virtanen, "Semi-empirical model for SEGR prediction," *IEEE Trans. Nucl. Sci*, vol. 60, no. 4, pp. 2660–2665, 2013.

[5] A. Virtanen, A. Javanainen, H. Kettunen, A. Pirojenko, I. Riihimäki, and K. Ranttila, "RADiation Effects Facility at JYFL." [Online]. Available: http://www.jyu.fi/accelerator/radef

[6] J. F. Ziegler, J. P. Biersack, M. Ziegler, D. J. Marwick, G. A. Cuomo, W. A. Porter, and S. A. Harrison, "SRIM 2013 code," 1984-2013. [Online]. Available: http://www.srim.org

[7] G. C. Messenger and M. S. Ash, *The Effects of Radiation on Electronic Systems*. Springer, 1992.

[8] S. M. Sze, *Physics of Semiconductor Devices*. New York: John Wiley and Sons, Inc., 1981.

[9] S. Suyama, A. Okamoto, T. Serikawa, and H. Tanigawa, "Electrical conduction and dielectric breakdown in sputter-deposited silicon dioxide films on silicon," *Journal of Applied Physics*, vol. 62, no. 6, pp. 2360–2363, 1987. [Online]. Available: http://link.aip.org/link/?JAP/62/2360/1

[10] M. J. Beck, B. R. Tuttle, R. D. Schrimpf, D. M. Fleetwood, and S. T. Pantelides, "Atomic displacement effects in single-event gate rupture," *IEEE Trans. Nucl. Sci*, vol. 55, no. 6, pp. 3025 –3031, dec. 2008.

[11] S. J. Bijlsma, H. Van Kranenburg, K. J. Nieuwesteeg, M. G. Pitt, and J. F. Verweij, "Electrical breakdown of amorphous hydrogenated silicon rich silicon nitride thin film diodes," *IEEE Trans. Electron Devices*, vol. 43, no. 9, pp. 1592–1601, 1996.

[12] I. S. Grant and W. R. Phillips, *Electromagnetism – 2nd ed.* John Wiley and Sons, Inc., 1990.